Available online at www.sciencedirect.com
SCIENCE DIRECT®
Ultrasonics 42 (2004) 1053–1059
Ultrasonics
www.elsevier.com/locate/ultras

Propagation of initially bi-harmonic sound waves in a 1D semi-infinite medium with hysteretic non-linearity

V. Aleshin [a,b,*], V. Gusev [c], V. Zaitsev [d]

[a] Laboratoire d'Acoustique, UMR—CNRS 6613, Faculté des Sciences, Université du Maine, av. O. Messiaen, 72085 Le Mans, France
[b] Interdisciplinary Research Center, Katholieke Universiteit Leuven (Campus Kortrijk), Etienne Sabbelaan 53, 8500 Kortrijk, Belgium
[c] Université du Maine, 72085 Le Mans, France
[d] Institute of Applied Physics, Russian Academy of Sciences, Uljanova St. 46, Nyzhnyi, 603950 Novgorod, Russia

Abstract

Materials with hysteretic non-linearity have the property of memorizing specific previous extrema in the stress/strain loading history. Because of this complexity, the analytical theory describing the non-linear evolution of acoustic waves in such materials is currently restricted to simplex wave propagation processes with a single minimum and a single maximum over a wave period. In the present paper a numerical model is presented which is valid for an arbitrary strain wave profile, and the results for the frequency-mixing process in acoustic waves composed initially of two harmonic frequency components are analyzed. The model simulations demonstrate that an initially complex wave transforms into a simplex wave during propagation. In addition, we have studied the mutual influence of the initial frequency components, and we have found regimes of induced absorption and induced transparency.

Keywords: Hysteretic non-linearity; Frequency mixing; Induced transparency; Non-linear wave evolution

1. Introduction

Acoustic experiments conducted in different types of materials (including, for example, polycrystalline metals [1–4], rocks [5–8] and ceramics [9]) lead to the conclusion on the universality of hysteresis of non-linear properties in the sense that hysteresis is characteristic of a large class of micro-inhomogeneous materials [2,10]. As a result of hysteresis, these materials have the fascinating property to memorize their acoustical loading history [11,12]. In particular, the material always "remembers" at least the extremum previous to the current condition, as well as the absolute maximum and the absolute minimum of the loading history.

Both end-point memory and hysteretic non-linearity can be successfully modelled in a phenomenological manner by using the so-called Preisach–Mayergoyz (PM) space formalism [13–16]. In the PM-space approach it is assumed that the response of a material to external excitation is a linear superposition of the individual responses of hysteretic mechanical elements. These elements act like triggers, i.e. they can be found in one of two states ("open" or "closed").

Exact analytical solutions for the propagation of non-linear waves in materials with hysteretic non-linearity are obtained [17–19] for the so-called "simplex" waves [20], i.e. periodic waves with a single maximum and a single minimum over a period. Qualitatively this was possible because there were only two end points (extrema) to be kept in memory during the wave profile transformation. However, if an acoustic wave contains additional local extrema apart from the absolute extrema ("complex" wave [20]), the problem of memorizing and erasing the end-points during the process of wave propagation becomes hardly tractable in an analytical formalism. This is exactly the point at which numerical modelling can help.

In the present paper we develop a numerical scheme for the evaluation of non-linear propagation of an

* Corresponding author. Address: Interdisciplinary Research Center, Katholieke Universiteit Leuven (Campus Kortrijk), Etienne Sabbelaan 53, 8500 Kortrijk, Belgium. Tel.: +32-56-24-6036.
E-mail address: aleshinv@mail.ru (V. Aleshin).

0041-624X/$ - see front matter © 2003 Elsevier B.V. All rights reserved.
doi:10.1016/j.ultras.2003.12.023

arbitrary acoustic signal, and present the results of this simulation in the case of an initially bi-harmonic signal, i.e., the acoustic wave at the boundary is composed of two harmonic waves at a fundamental frequency (ω) and its doubled frequency (2ω).

2. Evolution equation for a medium with hysteretic nonlinearity and its solution

Using the well-known method of a slowly varying wave profile (multiple time-scale technique) described, for example, in [21], we arrive at the "shortened" (evolution) equation for the slowly varying strain profile $s \approx \partial u/\partial x$ while propagating in the positive direction of the x-axis

$$\frac{\partial s}{\partial x} + v(x,\tau)\frac{\partial s}{\partial \tau} = 0. \tag{1}$$

Here $\tau = t - x/c_0$ denotes the "fast" retarded time, x is the "slow" evolution coordinate and

$$v(x,\tau) = -\frac{1}{2\rho_0 c_0^3}\frac{\partial \sigma_{\mathrm{H}}}{\partial s}, \tag{2}$$

where c_0 is the sound velocity, ρ_0 is density and σ_{H} is a contribution to the stress due to the presence of hysteretic elements.

In order to complete the model one should introduce an appropriate stress–strain relationship at this point. Following the ideas of the Preisach–Mayergoyz space formalism we assume here that the non-linear contribution to stress can be represented by a linear superposition of the contributions σ_{M} from a statistical ensemble of individual hysteretic mechanical elements located at position x:

$$\sigma_{\mathrm{H}}(s(x,\tau)) = \sum_{\mathrm{M}\in x}\sigma_{\mathrm{M}}. \tag{3}$$

Here the subscript M denotes the mechanical elements in the elementary volume at a coordinate x.

By considering the PM formalism, we replace the study of a complicated system consisting of multiple microscopic cracks (or defects) with the consideration of fictional elements, that can be found in one of two states: "open" or "closed" (we will denote these states as $S(\mathrm{M}) =$ "O" and $S(\mathrm{M}) =$ "C", respectively). The parameters of such an element are σ_{c}, σ_{o}, s_{c}, s_{o} (see Fig. 1). Here s_{o} is the strain value at which the element opens while we increase s, and s_{c} is the value needed to close it if strain decreases ($s_{\mathrm{c}} < s_{\mathrm{o}}$).

In order to evaluate the derivative $\partial\sigma_{\mathrm{H}}/\partial s = \sum_{\mathrm{M}\in x}\partial\sigma_{\mathrm{M}}/\partial s$ one needs to differentiate the curve plotted in Fig. 1. Mathematically, we obtain (with $\delta(s) = \infty$ if $s = 0$, $\delta(s) = 0$ if $s \neq 0$, and $\Delta\sigma = \sigma_{\mathrm{c}} - \sigma_{\mathrm{o}}$)

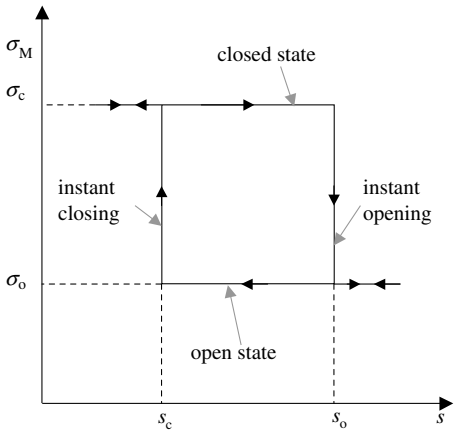

Fig. 1. Model of an individual hysteretic element M. The element is parameterized by the values of $s_{\mathrm{o}}, s_{\mathrm{c}}$ and $\Delta\sigma = \sigma_{\mathrm{c}} - \sigma_{\mathrm{o}}$.

$$\frac{\partial \sigma_{\mathrm{M}}}{\partial s} = -\Delta\sigma\begin{cases}\delta(s - s_{\mathrm{o}}), & \text{if } S(\mathrm{M}) = \mathrm{C}, \quad \partial s/\partial\tau > 0\\ \delta(s - s_{\mathrm{c}}), & \text{if } S(\mathrm{M}) = \mathrm{O}, \quad \partial s/\partial\tau < 0\\ 0, & \text{if } S(\mathrm{M}) = \mathrm{C}, \quad \partial s/\partial\tau < 0\\ 0, & \text{if } S(\mathrm{M}) = \mathrm{O}, \quad \partial s/\partial\tau > 0.\end{cases} \tag{4}$$

By substituting this expression in Eq. (3), one can calculate $v(x,\tau)$ using Eq. (2). Note that at each value of strain and after calculation of the derivative given by Eq. (4), we must keep track of the state $S(\mathrm{M})$ of each hysteretic mechanical element. Therefore we have to reassign $S(\mathrm{M})$ to "O" in the first case considered in Eq. (4) when s becomes larger than s_{o} and to "C" in the second case when s becomes smaller than s_{c} In other words, the state $S(\mathrm{M})$ of an element M depends not only on the current value of strain but also on the strain rate:

$$S(\mathrm{M}) = \begin{cases}\text{"O"}, & \text{if } s_{\mathrm{o}} \leqslant s\\ \text{"O"}, & \text{if } s_{\mathrm{c}} \leqslant s \leqslant s_{\mathrm{o}}, \quad \partial s/\partial\tau < 0\\ \text{"C"}, & \text{if } s \leqslant s_{\mathrm{c}}\\ \text{"C"}, & \text{if } s_{\mathrm{c}} \leqslant s \leqslant s_{\mathrm{o}}, \quad \partial s/\partial\tau > 0\end{cases}, \tag{5}$$

as it is illustrated in Fig. 1. Here one should stress the principal feature of the system under study: only the elements changing their state under a current s contribute to stress variation.

For simplicity we will consider $\Delta\sigma = \sigma_{\mathrm{o}} - \sigma_{\mathrm{c}}$ to be equal for all the elements and independent of x. In addition we assume a uniform distribution $f(s_{\mathrm{o}}, s_{\mathrm{c}}) = f_0 = \text{const}$ of hysteretic mechanical elements within the PM space. This formalism enables us to interpret $f(s_{\mathrm{o}}, s_{\mathrm{c}})\mathrm{d}s_{\mathrm{o}}\mathrm{d}s_{\mathrm{c}}$ as the number of mechanical elements in the PM rectangle $(s_{\mathrm{o}}, s_{\mathrm{o}} + \mathrm{d}s_{\mathrm{o}}) \times (s_{\mathrm{c}}, s_{\mathrm{c}} + \mathrm{d}s_{\mathrm{c}})$.

Making use of the above simplifications and replacing the summation over all elements in Eq. (3) with an integration over the entire PM space, we obtain the following expression:

$$\frac{\partial\sigma_{\mathrm{H}}}{\partial s} = \int_{-\infty}^{+\infty} \mathrm{d}s_{\mathrm{c}} \int_{-\infty}^{+\infty} \mathrm{d}s_{\mathrm{o}} \frac{\partial\sigma_{\mathrm{M}}}{\partial s} f(s_{\mathrm{o}}, s_{\mathrm{c}}) = f_0 \int_{-\infty}^{s_{\mathrm{o}}} \mathrm{d}s_{\mathrm{c}} \int_{s_{\mathrm{c}}}^{+\infty} \mathrm{d}s_{\mathrm{o}} \frac{\partial\sigma_{\mathrm{M}}}{\partial s} \tag{6}$$

The latter expression, together with Eqs. (1), (2), (4) and (5) describe the propagation of a strain wave in a material with hysteretic elements.

To completely solve the problem, we consider the boundary condition $s(x=0,\tau) = s_{\mathrm{b}}(\tau)$ and an initial condition for the state of the elements $S(\mathrm{M})|_{\tau=0} = S_0(\mathrm{M})$, that can, in general, depend on x. This initial state is usually unknown in a real situation, but for any given distance x after a transition time of several cycles of strain oscillation the stored initial memory will be lost and the solution will become strictly periodical.

A graphical illustration of the hysteretic element switching procedure is plotted in Fig. 2(a), which contains a series of "snap-shots" in PM-space, corresponding to different points (0–15) of the strain curve $s(\tau)$ in Fig. 2(b). The strain evolution presented in Fig. 2(b) is chosen rather arbitrary.

Now let us examine the evolution of $v(x,\tau)$ (Eq. (2)). To illustrate the process of switching we have plotted a more detailed visualization in Fig. 3. After passing some

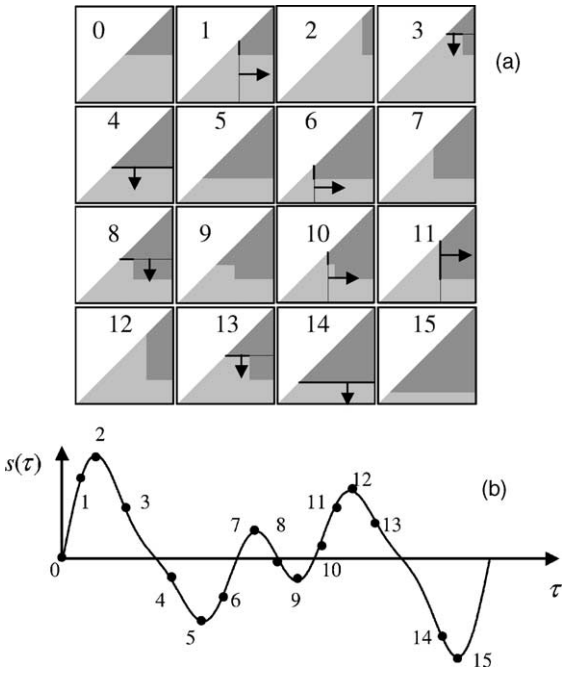

Fig. 2. Illustration of the switching procedure in PM space. The pictures 0–15 (a) are patterns in the $(s_{\mathrm{o}}, s_{\mathrm{c}})$-PM-space corresponding to the points 0–15 on the strain curve $s(\tau)$ below (b). The arrows indicate the direction of switching. Areas containing open elements are plotted in light gray, areas containing the closed elements are dark gray. The "switching lines" are marked by thin lines in each portrait, the "switching sections" are marked by the thicker portion of the "switching line". The pictures 2, 5, 7, 9, 12, 15 correspond to end points (absolute and local extrema of $s(\tau)$).

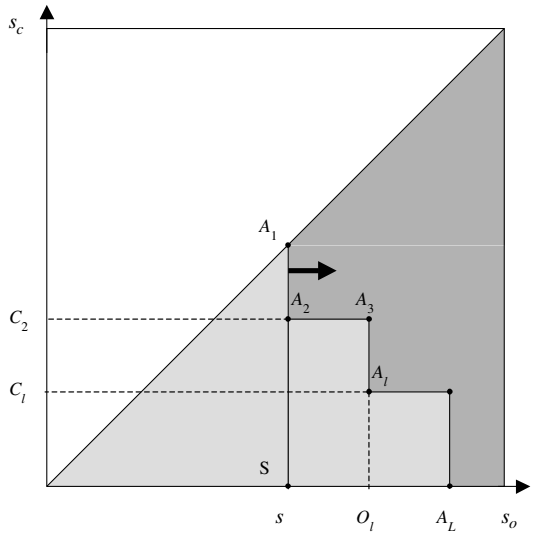

Fig. 3. Parameterization of the PM-space configuration by the corner points $A_1, A_2, \ldots, A_l \ldots A_L$ of the boundary between open (light gray) and closed (dark gray) areas. The "switching line" is the vertical interval $A_1\mathrm{S}$, the "switching section" corresponds to the portion A_1A_2.

extrema of $s(\tau)$, any possible PM configuration will contain two areas (one area with fully open elements, and one area with only fully closed elements), separated by a broken line $A_1A_2 \ldots A_L$. The coordinates of a node A_l $(l = 1, 2, \ldots, L)$ are denoted as $(\mathrm{O}_l, \mathrm{C}_l)$. The current value of strain s determines the switching line $A_1\mathrm{S}$. In the illustrated case this line is vertical and performs an "opening"-operation, $\partial s/\partial\tau > 0$. The reasoning is analogous for "closing"-operations (see later). If $\partial s/\partial\tau > 0$, then $\partial\sigma_{\mathrm{M}}/\partial s = -\Delta\sigma\delta(s - s_{\mathrm{o}})$ or $\partial\sigma_{\mathrm{M}}/\partial s = 0$ (cf. Eq. (4)). Hence Eq. (6) reads:

$$\frac{\partial\sigma_{\mathrm{H}}}{\partial s} = f_0 \int_{-\infty}^{s_{\mathrm{o}}} \mathrm{d}s_{\mathrm{c}} \int_{s_{\mathrm{c}}}^{+\infty} \frac{\partial\sigma_{\mathrm{M}}}{\partial s} \mathrm{d}s_{\mathrm{o}} = f_0\Delta\sigma \int_{-\infty}^{s} \Omega\,\mathrm{d}s_{\mathrm{c}}, \tag{7}$$

where $\Omega = -1$ if $\partial\sigma_{\mathrm{M}}/\partial s = -\Delta\sigma\delta(s - s_{\mathrm{o}})$, and $\Omega = 0$ if $\partial\sigma_{\mathrm{M}}/\partial s = 0$. As a result, the integration along the switching line $A_1\mathrm{S}$ (i.e. $-\infty < s_{\mathrm{c}} < s$) in Eq. (7) reduces to the integration along the "switching section" A_1A_2 (see Fig. 3), i.e.:

$$\frac{\partial\sigma_{\mathrm{H}}}{\partial s} = f_0\Delta\sigma \int_{-\infty}^{s} \Omega\,\mathrm{d}s_{\mathrm{c}} = f_0\Delta\sigma \int_{C_2}^{s} (-1)\,\mathrm{d}s_{\mathrm{c}} = -f_0\Delta\sigma(s - C_2). \tag{8}$$

In the case $\partial s/\partial\tau < 0$ (closing-operation) the above Eq. (8) is analogous:

$$\frac{\partial\sigma_{\mathrm{H}}}{\partial s} = -f_0\Delta\sigma(O_2 - s). \tag{9}$$

After deriving the initial function v from the initial conditions, the procedure of building the subsequent solution in space and time becomes evident: we numerically solve Eq. (1) using central differences, update and store the coordinates of the points A_l in PM-space at

each step, and use them to calculate $v(x,\tau)$ according to Eqs. (8) and (9).

3. Results of the numerical solution of the evolution equation

Before we discuss the results, we remark that all variables have been normalized: $s' = s/s_0$, $\tau' = f\tau$, $x' = x/x_{nl}$, where s_0 is a characteristic strain value, f is a fundamental frequency, and $x_{nl} = \left(2\rho_0 c_0^3\right)/(fs_0\Delta\sigma f_0)$. In the following, the primes will be omitted everywhere.

To estimate the precision provided by the numerical method we have compared numerical results for a pure harmonic excitation (boundary condition $s(x=0,\tau) = \sin 2\pi$) with the existing analytical solution [17]. For 8192 points per τ-period we found the precision in the harmonics amplitudes, defined by

$$s(x,\tau) = \sum_{n=0}^{\infty} Z_n(x)\,\sin(2\pi n\tau + \psi_n(x)), \tag{10}$$

within 0.03%, 0.46%, 0.47%, and 1.3% for the third, fifth, seventh and ninth harmonics, respectively. (It is well-known that even harmonics are not generated in a purely hysteretic case.)

However, our purpose is to treat more complicated excitation signals containing two or more extrema per period ("complex" waves). For instance, the signal:

$$s(x=0,\tau) = A_1 \sin 2\pi\tau + A_2 \sin 4\pi\tau, \tag{11}$$

is simplex (one pair of extrema per period) when $A_2 < A_1/2$ and complex in the opposite case.

Figs. 4 and 5 represent the strain profiles and their spectra for typical simplex and complex processes. The remarkable feature observed in the spectrum evolution is the faster initial growth of the 4ω-wave-component in comparison with the 3ω-component. At first glance this looks unexpectedly because the efficiency of the process $(\omega) + 2(\omega) = 3\omega$ is proportional to A_1^2, while the efficiency of the process of the 4ω-component generation $(2\omega) + 2(\omega) = 4\omega$ (where one phonon of the 2ω-wave is combined with two phonons of the ω-wave) is proportional to A_1A_2, and this is normally lower than A_1^2 since we have taken $A_2 \ll A_1$. However, it should be taken into account that in the presence of the 2ω-wave there is an additional process of direct excitation of the third harmonic: $-(\omega) + 2(2\omega) = 3\omega$, where two phonons of the 2ω-wave are combined with a phonon of the ω-wave. Clearly, if the latter process is acting in anti-phase to the process $(\omega) + 2(\omega) = 3\omega$, its existence could be responsible for the decrease of the 3ω-amplitude in the presence of the 2ω-wave (Figs. 4 and 5) in comparison with the case of a purely monochromatic input.

Another important feature which can be extracted from the analysis of the wave profile transformation shown in Fig. 5(a) is the gradual transformation of a complex wave into a simplex wave with increasing propagation distance. The local maximum disappears due to the hysteretic absorption. Hysteretic absorption has a very clear "geometrical" manifestation that can be observed near the wave extrema. In fact, similar to the case of a pure sinusoidal wave [17,18] (or to the case of the acoustic pulses [19]) the leading part of the wave profile near the extremum is always delayed due to non-linear effects relative to the trailing part. An extremum itself is the intersection point of these increasing and decreasing (or vice versa) parts of the profile where the leading part moves near the extremum in the direction of the trailing part [17]. Indeed, the formal mathematics demonstrates that the non-linear contribution to sound

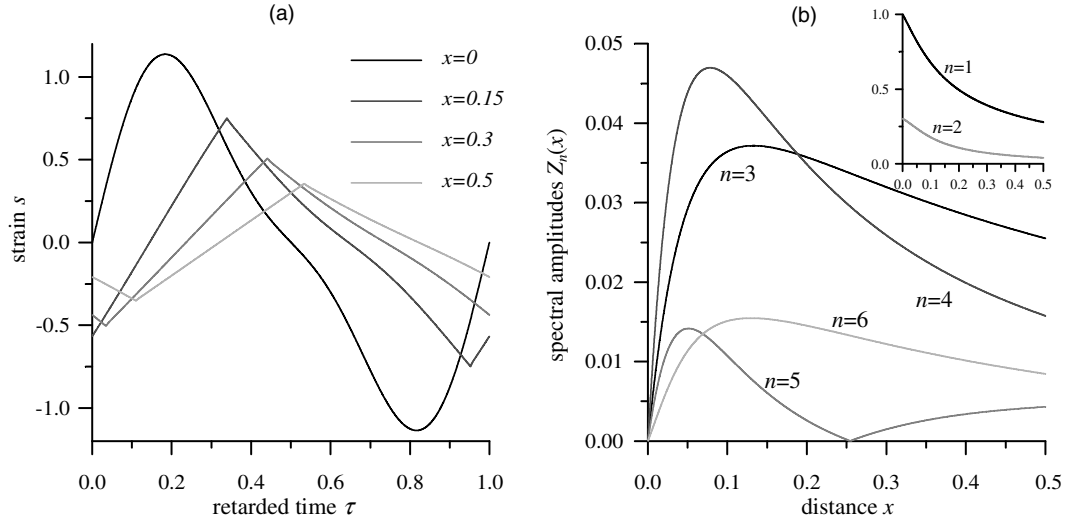

Fig. 4. Non-linear distortion of a bi-harmonic strain wave signal (a), and the distance dependence of the spectral amplitudes $Z_n(x)$ for different frequencies $n\omega$ (b). The initial signal equals $s(x=0,\tau) = A_1 \sin 2\pi\tau + A_2 \sin 4\pi\tau$, with $A_1 = 1$, $A_2 = 0.2$ ("simplex" profile).

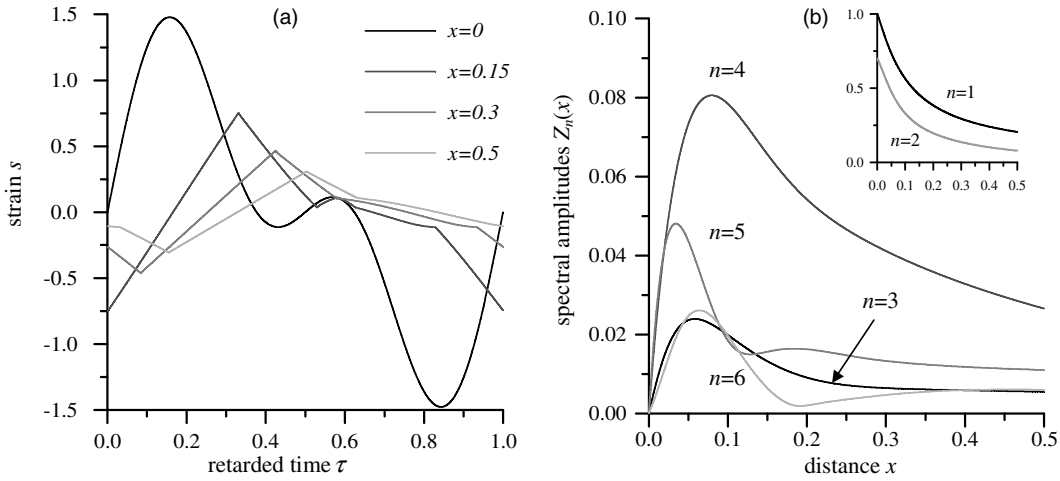

Fig. 5. Non-linear distortion of a bi-harmonic strain wave signal (a), and the distance dependence of the spectral amplitudes $Z_n(x)$ for different frequencies $n\omega$ (b). The initial signal equals $s(x=0,\tau)=A_1\sin 2\pi\tau + A_2\sin 4\pi\tau$, with $A_1=1$, $A_2=0.7$ (“complex” profile).

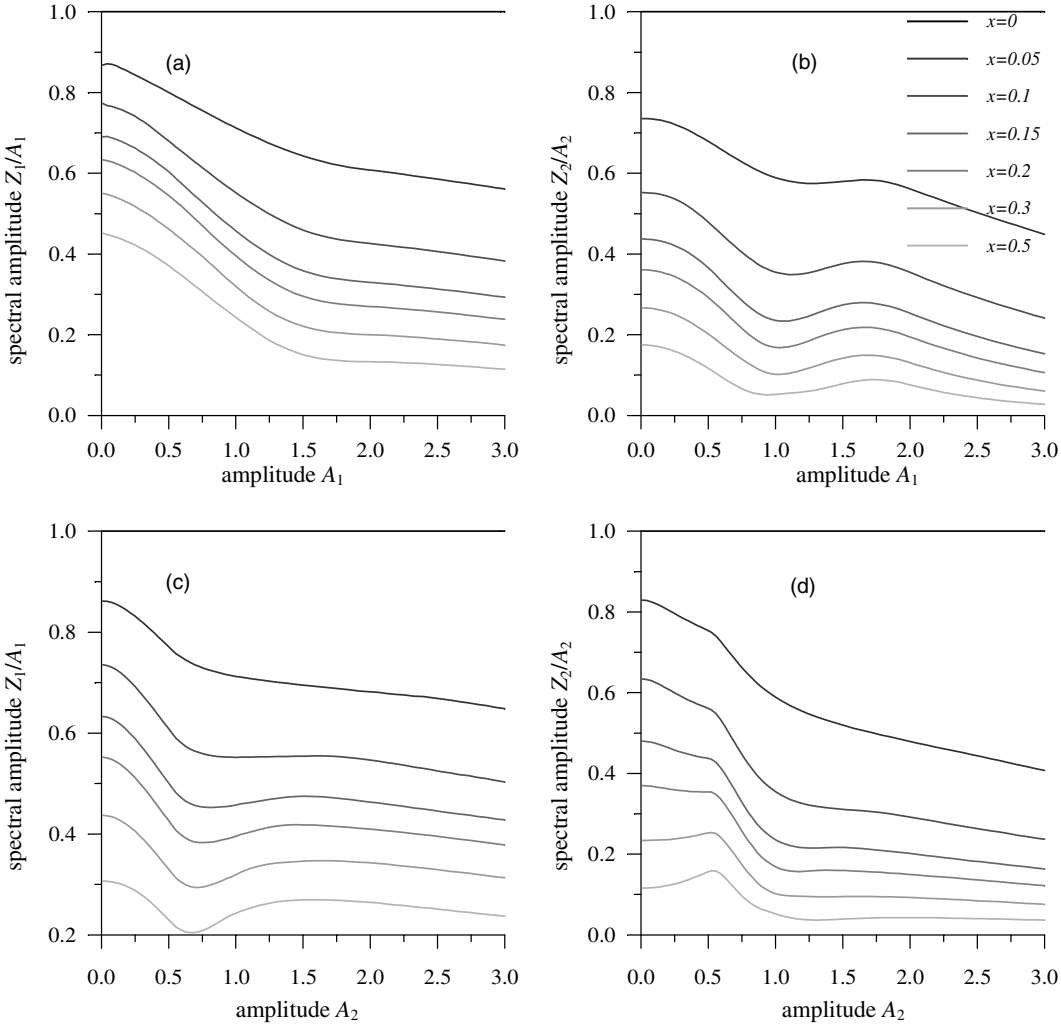

Fig. 6. Normalized spectral amplitudes Z_1/A_1 (a, c) and Z_2/A_2 (b, d) for different distance x as function of the amplitude A_1 ($A_2=1=\text{const}$) (a, b) and of A_2 ($A_1=1=\text{const}$) (c, d), calculated for the initial signal $s(x=0,\tau)=A_1\sin 2\pi\tau + A_2\sin 4\pi\tau$.

velocity is always negative just before reaching an extremum and is equal to zero just after the extremum. The continuous mutual "penetration" of these leading and trailing parts leads to the observed reduction of the strain amplitude (compare for example the profiles at $x = 0$ and $x = 0.5$ in Fig. 4(a)).

Though the obtained results concerning the higher harmonics are interesting, the higher harmonics excited in the multiple-phonon processes are usually small in comparison with fundamental ones (less than 5%). Consequently, it may be more instructive to analyze the mutual influence of the initial wave components in the process of frequency mixing. In Fig. 6, we illustrate the dependence of the amplitude of one wave component on the amplitude of the other one at different distances from the boundary. A careful examination of the results in Fig. 6 leads to the conclusion that at short propagation distances ($x = 0.05$) the increase in the amplitude of either the ω-component (A_1) or the 2ω-component (A_2) generally induces additional absorption ($\partial(Z_1/A_1)/\partial A_1 < 0$, $\partial(Z_1/A_1)/\partial A_2 < 0$, $\partial(Z_2/A_2)/\partial A_2 < 0$), with $Z_{1,2}$ defined in Eq. (10)). Only the dependence of the 2ω-wave amplitude on the amplitude of the ω-wave exhibits a regime of the induced transparency ($\partial(Z_2/A_2)/\partial A_1 > 0$) in the neighborhood of $A_1 \approx 1.5$ (Fig. 6(b)). At larger propagation distances this induced transparency regime becomes more pronounced, and intervals of induced transparency are also predicted for the influence of 2ω-wave on the ω-component as well (Fig. 6(c), for $x \geqslant 0.2$ and $A_2 \approx 1$). Moreover, self-induced transparency can be observed for the 2ω-component as function of the 2ω-wave amplitude at sufficiently large distances (Fig. 6(d), $\partial(Z_2/A_2)/\partial A_2 > 0$ for $x \geqslant 0.3$ and $A_2 \leqslant 0.5$).

The numerical predictions of the existence of induced transparency effects at short propagation distances indicate that these effects (at least near the boundary) are not due to a simple wave spectrum transformation but must be attributed to the peculiar features of local non-linear hysteretic absorption in the two-frequency mixing process. To verify this, we should analyze the local hysteretic absorption of both ω-and 2ω-oscillations at the boundary $x = 0$. Fortunately, in the case of $s(x = 0, \tau) = A_1 \cos 2\pi\tau + A_2 \cos 4\pi\tau$, it is possible to develop an analytical description of the local hysteretic absorption in addition to numerical treatment. The analytical results confirm the effects predicted numerically in this paper and provide additional insight in the physics of frequency mixing in materials with hysteretic quadratic non-linearity [22]. A detailed analysis will be presented in [23].

4. Conclusions

The numerical framework is developed for the analysis of plane acoustic wave propagation in non-linear hysteretic materials. A numerical investigation of the ω- and 2ω-wave mixing process in materials with hysteretic quadratic non-linearity revealed multiple complex phenomena due to hysteresis and memory in the considered materials.

It was found that for certain combinations of the ω- and 2ω- input waves the efficiency of the fourth harmonic (4ω) component generation can exceed the efficiency of the third harmonic (3ω) excitation. In addition, the transformation of a complex wave into a simplex wave during non-linear propagation has been demonstrated.

Peculiar regimes of induced transparency (for which an increasing amplitude of the ω (2ω)-wave leads to a reduction of the absorption of 2ω (ω)-wave) are predicted. Also, the existence of a regime of self-induced transparency (for which in the presence of the ω-wave an increasing amplitude of the 2ω-wave induces a reduction of the absorption of the 2ω-wave) has been demonstrated.

The obtained results are expected to find applications in the non-destructive evaluation of hysteretic materials and in seismology.

Acknowledgements

One of us (V.A.) gratefully acknowledges the Fellowship from the University of Maine (France, 2001–2002) and the Grant G.0206.02 from the Foundation for Scientific Research of Flanders (Belgium, 2002–2003). V.Z. acknowledges partial support by RFBR (grant 02-02-16237).

References

[1] V.E. Nazarov, L.A. Ostrovsky, I.A. Soustova, A.M. Sutin, Sov. Phys. Acoust. 34 (1988) 284.
[2] V.E. Nazarov, L.A. Ostrovsky, I.A. Soustova, A.M. Sutin, Phys. Earth Planet. Inter. 50 (1988) 65.
[3] V.E. Nazarov, Sov. Phys. Acoust. 37 (1991) 75.
[4] V.E. Nazarov, J. Acoust. Soc. Am. 107 (2000) 1915.
[5] V.E. Nazarov, S.V. Zimenkov, Acoust. Lett. 16 (1993) 218.
[6] P.A. Johnson, B. Zinszner, P.N.J. Rasolofosaon, J. Geophys. Res. 101 (1996) 11553.
[7] B. Zinszner, P.A. Johnson, P.N.J. Rasolofosaon, J. Geophys. Res. 102 (1997) 8105.
[8] V.E. Nazarov, A.V. Radostin, I.A. Soustova, Sov. Phys. Acoust. 48 (2002) 85.
[9] J.K. Na, M.A. Breazeale, J. Acoust. Soc. Am. 95 (1994) 3213.
[10] R.A. Guyer, P.A. Johnson, Phys. Today 52 (1999) 30.
[11] D.J. Holcomb, J. Geophys. Res. 86 (1981) 6235.
[12] R.A. Guyer, K.R. McCall, G.N. Boitnott, Phys. Rev. Lett. 74 (1995) 491.
[13] F. Preisach, Z. Phys. 94 (1935) 277.
[14] I.D. Mayergoyz, J. Appl. Phys. 57 (1985) 3803.

[15] I.D. Mayergoyz, Phys. Rev. Lett. 56 (1986) 1518.
[16] M.A. Krasnosel'skii, A.V. Pokrovskii, Systems with Hysteresis, Nauka/Springer, Moscow/Berlin, 1983/1989.
[17] V. Gusev, C. Glorieux, W. Lauriks, J. Thoen, Phys. Lett. A 32 (1997) 77.
[18] V. Gusev, W. Lauriks, J. Thoen, J. Acoust. Soc. Am. 103 (1998) 3216.
[19] V. Gusev, J. Acoust. Soc. Am. 107 (2000) 3047.
[20] K.E.-A. Van Den Abeele, P.A. Johnson, R.A. Guyer, K.R. McCall, J. Acoust. Soc. Am. 101 (1997) 1885.
[21] O.V. Rudenko, S.I. Soluyan, Theoretical Foundations of Nonlinear Acoustics, Consultants Bureau, New York, 1976.
[22] V. Gusev, Phys. Lett. A 271 (2000) 100.
[23] V. Aleshin, V. Gusev, V. Zaitsev, J. Comp. Ac. (in press).